Journal of Achievements in Materials and Manufacturing Engineering
VOLUME 27
ISSUE 2
April
2008

Finite element analysis of elliptic cup deep drawing of magnesium alloy sheet

T.S. Yang *
Department of Mechanical and Computer-Aided Engineering,
National Formosa University; 64 Wunhau Rd., Huwei, 632 Yunlin, Taiwan
* Corresponding author: E-mail address: tsyang@nfu.edu.tw

Received 22.01.2008; published in revised form 01.04.2008

Materials

ABSTRACT

Purpose: In magnesium alloy sheet products have been attracting more and more attention in recent years because of their application potentials as coverings of portable electrical devices and automotive panels. Thus this paper focus on the deep drawing process of magnesium alloy sheet.
Design/methodology/approach: The FEM soft ware DEFORM-3D is used to investigate the mateial flow character during the elliptic cup deep drawing of magnesium alloy sheet at elevated temperatures.
Findings: Investigate the effective stress and forming load under various process parameter conditions, including the profile radius of die, the clearance between die cavity and punch, the blank holding force and working temperature during the elliptic cup deep drawing of magnesium AZ31 alloy sheet.
Research limitations/implications: The initial blank's shape design and forming limit analysis of the elliptic cup deep drawing of magnesium AZ31 alloy sheet will be continued for future research.
Originality/value: The original value of this paper is the finite element method is used to investigate the material flow character, forming load, stress and strain distribution during the the elliptic cup deep drawing of magnesium alloy sheet at elevated temperatures.
Keywords: Magnesium alloy sheet; Finite element analysis; Deep drawing; Elliptic cup

1. Introduction

Due to its lightweight and high specific strength, high thermal conductivity, good electromagnetic shielding capability and recycle, Magnesium (Mg) alloys are nowadays very attractive in many fields (aerospace, automobile and electronic industries). Deep drawing is a process for shaping flat sheets into cup-shaped articles without fracture or excessive localized thinning. The design and control of a deep drawing process depends not only on the workpiece material, but also on the condition at the tool- workpiece interface, the mechanics of plastic deformation and the equipment used. There are many researches [1-4] focus on the effects of process or material parameters on the on deep drawing process.

However, The Mg alloy AZ31 sheet usually exhibits limited ductility at room temperature because of its hexagonal close-packed (HCP) structure. Many recent research activities have pointed out that the Mg alloy AZ31 is characterized by a good formability at elevated temperature [5–11]. In addition, the fabrication of excellent sheet is important to improve its formability. During the design of deep drawing processes, numerical simulation which can predicate material flow trend, stress and strain distribution, can help to determine the optimal processing parameters and explore novel forming technique [12,13].

In this paper, the FEM soft ware DEFORM-3D is used to simulate the ellipic cup deep drawing of Mg metal sheet at elevated temperatures. A finite element method is also used to investigate the effective stress and forming load under various process parameter conditions, including the profile radius of die, the clearance between die cavity and punch, the blank holding force and working temperature.

2. Finite element molding

This study applies commercial finite element code DEFORM-3D [14] to simulate the plastic deformation behavior during the helical gear forging process. The basic equations of the rigid-plastic finite element are as follows:

Equilibrium equation:

$$\sigma_{ij,j} = 0 \tag{1}$$

Compatibility and incompressibility equations:

$$\dot{\varepsilon}_{ij} = \frac{1}{2}\left(u_{i,j} + u_{j,i}\right), \quad \dot{\varepsilon}_v = u_{i,i} = 0 \tag{2}$$

Constitutive equations:

$$\sigma'_{ij} = \frac{2\bar{\sigma}}{3\dot{\bar{\varepsilon}}}\dot{\varepsilon}_{ij}, \quad \bar{\sigma} = \sqrt{\frac{3}{2}\left(\sigma'_{ij}\sigma'_{ij}\right)}, \quad \dot{\bar{\varepsilon}} = \sqrt{\frac{3}{2}\left(\dot{\varepsilon}_{ij}\,\dot{\varepsilon}_{ij}\right)} \tag{3}$$

Boundary conditions:

$$\sigma_{ij}n_i = F_j \text{ on } S_F, \quad u_i = U_i \text{ on } S_U \tag{4}$$

where σ_{ij} and $\dot{\varepsilon}_{ij}$ are the stress and the strain rate, respectively, $\bar{\sigma}$ and $\dot{\bar{\varepsilon}}$ are the effective stress and the effective strain rate, respectively, F_j is the force on the boundary surface of S_F, and U_i is the deformation velocity on the boundary surface of S_U.The weak form of rigid-plastic FEM can be determined by applying the variational method to Eqs. (1) –(4), i.e.

$$\int_V \bar{\sigma}\delta\dot{\bar{\varepsilon}}\,dV + K\int_V \dot{\varepsilon}_V\delta\dot{\varepsilon}_V\,dV - \int_{SF} F_i\delta u_i dS = 0 \tag{5}$$

where V and S are the volume and the surface area of the material, respectively, and K is the penalty constant.

3. Results and discussions

A schematic diagram of the elliptic cup deep drawing process is shown in Fig. 1. An initially flat thin elliptic Mg metal sheet is placed onto a drawing die and an adequate pressure is applied to the blank holder. The punch moves down to make contact with the sheet and to draw it into a elliptic cup. Note that *a* is long axis of ellipic punch; *b* is short axis of ellipic punch; *c* is the clearance between punch and die; R_p is the profile radis of punch; R_d is the profile radis of die; P_b is the blanker holder force; T is working temperature. Yang and Hsu [15] shows the DEFORM-3D has reasonable accurate for the simulation of deep drawing process. Thus DEFORM-3D software is used in current simulation.

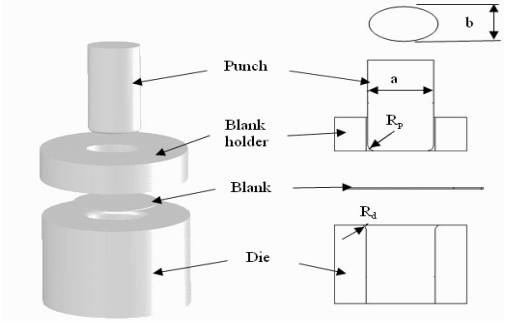

Fig. 1. Schematic diagram of elliptic cup deep drawing process

The present analysis adopt the following assumptions: (1) the punch, die and blank holder are rigid bodies; (2) the blank is a elastic-plastic material; and (3) the friction factors between the blank and the punch, die, and blank holder are constant. The blank is ellipic Mg metal sheet and the stress-strain relationship of Mg for different temperature is shown in Fig. 2; the long axis, short axis and thickness of blank is 80 mm, 50 mm and 1.0 mm, respectively. The workpiece is modeled using approximately 9200 nodes and 13900 elements. Coulomb friction coefficient is assumed as 0.01 at the interfaces between punch/workpiece and die/workpiece, and the punch velocity is 1.2 *mm/s*. Fig. 3 shows the effective stress and effective strain distribution under the condition of profile radius of die is 6 mm, blank holder force is 1500 N, clearance between punch and die is 1.6 mm and working temperature is 300°C. The maximum effective stress and effective strain occurs at the top edges of the product. The maximum value of effective stress is 60.0 MPa, while the maximum value of effective strain is 2.29. To investigate the effects of process parameters on the forming load, maximum effective stress of magnesium AZ31 alloy sheet, numerical analysis was performed for each change in these values.

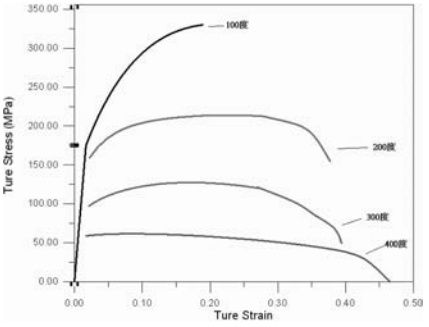

Fig. 2. Stress-strain relationship of magnesium AZ31 alloy sheet

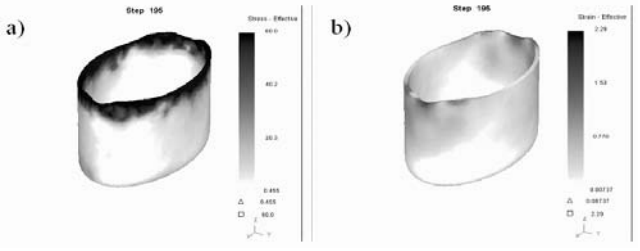

Fig. 3. Effective stress and effective strain distribution: a) effective stress distribution, b) effective strain distribution

3.1. Effect of the profile radius

Fig. 4 shows effects of the profile radius on forming load under the condition of P_h = 1500 N, c = 1.6 mm and T = 300°C. It appears that the smaller value of the profile radius of die would require more forming load to form the ellipic cup completely.

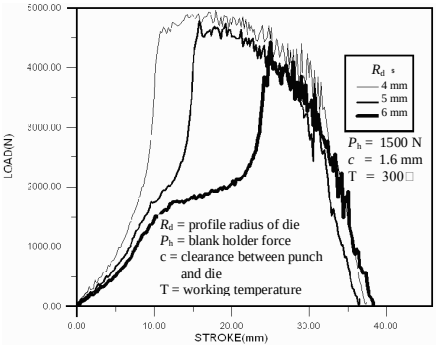

Fig. 4. Effect of profile radius of die on forming load

The maximum forming load decreases as the profile radius is increased. The maximum forming load is found to decrease from 4960 N to 4420 N over the profile radius range 4 mm $\leq R_d \leq$ 6mm. Fig. 5 shows the profile radius of die on maximum effective stress and maximum effective strain under the condition of blank holding force 1500 N, clearance between punch and die 1.6 mm, and working temparature 300°C. The maximum effective stress occurs at the top edges of the product. It can be seen that the values of maximum effective stress decrease as the profile radius of die increase. Specifically, the maximum effective stress reduces from 90.2 MPa to 60 MPa as the profile radius over the range 4 mm $\leq R_d \leq$ 6mm.

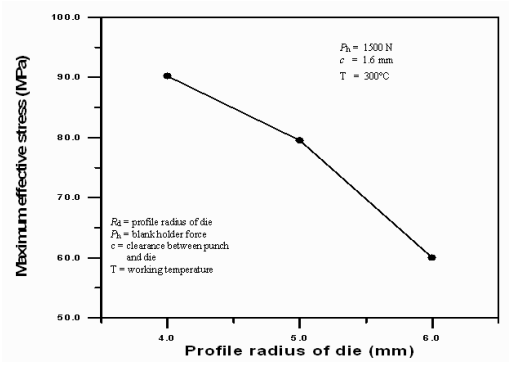

Fig. 5. Effect of profile radius of die on maximum effective stress

3.2. Effect of the blank holder force

Fig. 6 shows effects of the blank holder force on forming load under the condition of R_d = 6 mm, c = 1.6 mm and T = 300°C. It noted that the largerer value of the blank holder force would require more forming load to form the ellipic cup completely. The maximum forming load increases as the blank holder force is increased. The maximum forming load is found to increase from 4420 N to 5080 N over the profile radius range 1500 N $\leq P_h \leq$ 3500 N. Fig. 7 shows the blank holder force on maximum effective stress under the condition of profile radius of die 6 mm, clearance between punch and die 1.6 mm, and working temperature 300 ˚C. The maximum effective stress occurs at the top edges of the product. It can be seen that the values of maximum effective stress increase as the blank holder force increase. Specifically, the maximum effective stress increase from 60 MPa to 84.6 MPa as theblank holder force over the range 1500 N $\leq P_h \leq$ 3500 N.

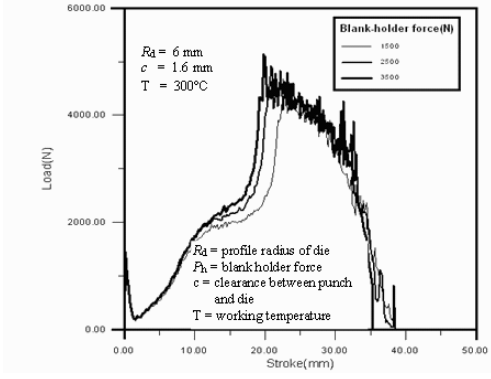

Fig. 6. Effect of blank holder force on forming load

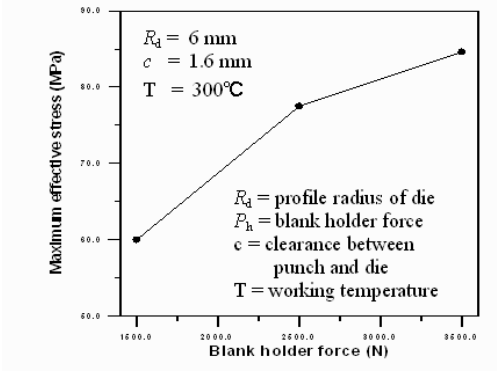

Fig. 7. Effect of blank holder force on maximum effective stress

3.3. Effect of the clearance between punch and die

Fig. 8 shows effects of the clearance between punch and die on forming load under the condition of R_d = 6 mm, P_h = 1500 N and T = 300°C. It is observed that the largerer value of the clearance between punch and die would require more forming load to form the ellipic cup completely. The maximum forming load decreases as the clearance between punch and die is increased. The maximum forming load is found to decrease from 5020 N to 4420 N over the profile radius range 1.2 mm $\leq c \leq$ 1.6mm. Fig. 9 shows the clearance between punch and die on maximum effective stress and strain under the condition of blank holding force 1500 N, profile radius of die 6 mm, and working temparature 300°C. The maximum effective stress occurs at the top edges of the product. The maximum effective stress is found to decrease from 84.1 MPa to 60 MPa over the range of clearance between punch and die 1.2 mm $\leq c \leq$ 1.6 mm.

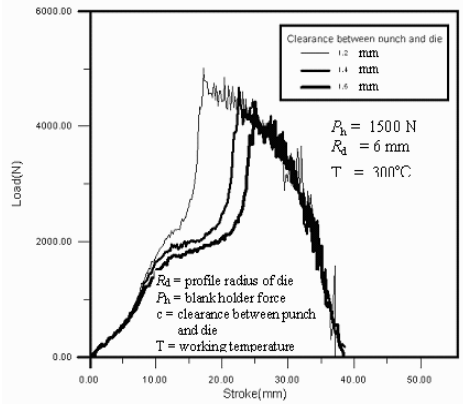

Fig. 8 Effect of clearance between punch and die on forming load

3.4. Effect of the working temperature

Fig. 10 shows effects of the working temperature on forming load under the condition of R_d = 6 mm, P_h = 1500 N and c = 1.6 mm. It is clear that the largerer value of the working temperature would require more forming load to form the ellipic cup completely. The maximum forming load decreases as the working temperature is increased. The maximum forming load is found to decrease from

12300 N to 4420 N over the working temperature range 100°C≤ $T \leq 300$ ˚C. Fig. 11 shows the working temperature on maximum effective stress under the condition of blank holding force 1500 N, profile radius of die 6 mm, and clearance between punch and die 1.6 mm. The maximum effective stress occurs at the top edges of the product. The maximum effective stress decrease from 179 MPa to 60 MPa over the working temperature range of 100 °C≤ $T \leq 300$ °C.

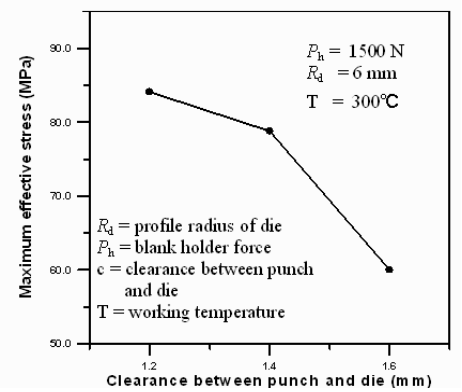

Fig. 9. Effect of clearance between punch and die on maximum

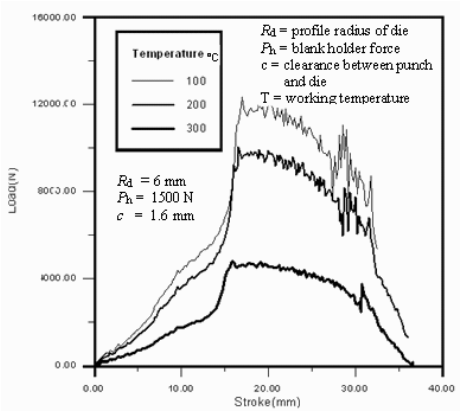

Fig. 10. Effect of working temperature on forming load

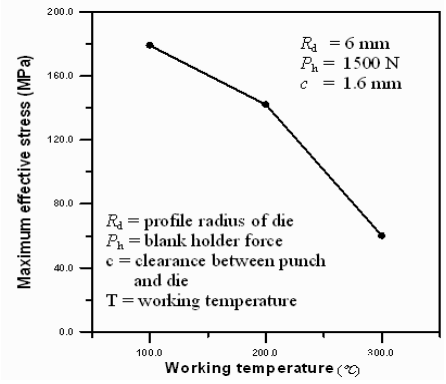

Fig. 11. Effect of working temperature on maximum effective stress

4. Conclusions

In this paper, the FEM soft ware DEFORM-3D is used to simulate the ellipic cup deep drawing of magnesium AZ31 alloy sheet at elevated temperatures. A finite element method is also used to investigate the effective stress and forming load under various process parameter conditions, including the profile radius of die, the clearance between die cavity and punch, the blank holding force and working temperature.

Acknowledgements

The author wish to thank the support from the National Science Council under grants NSC- 95-2221-E-150-015.

References

[1] R. Hill, A theory of the yielding and plastic flow of anisotropic metals, Proceedings of Royal Society of London, 1948, 193-281.
[2] F. Barlat, J. Lian, Plastic behavior and stretch ability of sheet metals. I. A yield function for orthotropic sheet under plane stress conditions, International Journal of Plasticity 5 (1989) 51-56.
[3] Y.Q. Liu, J.C. Wang, P. Hu, The numerical analysis of anisotropic sheet in deep-drawing processes, Journal of Materials Processing Technology 120 (2002) 45-52.
[4] A. Hrivnak, L. Sobotova, The influence of the deformation aging and conditions of stress on the properties of the deep drawing steel sheet, Journal of Materials Processing Technology 34 (1992) 425-430.
[5] S. Yoshihara, H. Nishimura, H. Yamamoto, K.I. Manabe, Formability enhancement in magnesium alloy stamping using a local heating and cooling technique, Journal of Materials Processing Technology 142 (2003) 609-613.
[6] S.H. Zhang, Y.C. Xu, Z.T. Wang, Q.L. Zhang, G. Palumbo, S. Pinto, L. Tricarico, Formability and process conditions of magnesium alloy sheets, Magnesium Science, Technology and Applications, Material Science Forum 488–489 (2005) 453-456.
[7] G. Palumbo, D. Sorgente, L. Tricarico, S.H. Zhang, W.T. Zheng, Numerical and experimental analysis of the Mg alloy formability when superimposing a thermal gradient, Journal of Achievements in Materials Manufacturing Engineering 14 (2006) 504-512.
[8] S.H. Zhang, K. Zhang, Y.C. Xua, Z.T. Wang, Y. Xua, Z.G. Wang, Deep-drawing of magnesium alloy sheets at warm temperatures, Journal of Materials Processing Technology 185 (2007) 147-151.
[9] F.K. Chen, T.B. Huang, C.K. Chang, Deep drawing of square cups with magnesium alloy AZ31 sheets, International Journal of Machine Tools and Manufacture 43 (2003) 1553-1559.
[10] G. Palumbo, D. Sorgente, L. Tricarico, S.H. Zhang, W.T. Zheng, Numerical and experimental investigations on the effect of the heating strategy and the punch speed on the warm deep drawing of magnesium alloy AZ31, Journal of Materials Processing Technology 191 (2007) 342-346.
[11] A. Wahab E. Morsy, K.I Manabe, Finite element analysis of magnesium AZ31 alloy sheet in warm deep-drawing process considering heat transfer effect, Materials Letters 60 (2006) 1866-1870.
[12] H. Palaniswam, G. Ngaile, T. Altan, Finite element simulation of magnesium alloy sheet forming at elevated temperatures, Journal of Materials Processing Technology 146 (2004) 52-60.
[13] H. Takuda, N. Hatta, Numerical analysis of formability of a commercially pure zirconium sheet in some sheet forming processes, Materials Science and Engineering A 242 (1998) 15–21.
[14] DEFORM-3D User's Manual, Version 8.0, Scientific Forming Technologies Corporation, Columbus, OH,. (2003)
[15] T.S. Yang and Y.C. Hsu, The Prediction of Earing and Design of initial Shape of Blank in Cylindrical Cup Drawing, Journal of Materials Science Forum 532-533 (2007) 865-868.